

# The Durham/UKST Galaxy Redshift Survey - III. Large Scale Structure via the 2-Point Correlation Function.

A. Ratcliffe<sup>1</sup>, T. Shanks<sup>1</sup>, Q.A. Parker<sup>2</sup> and R. Fong<sup>1</sup>

<sup>1</sup>*Physics Department, University of Durham, South Road, Durham, DH1 3LE.*

<sup>2</sup>*Anglo-Australian Observatory, Coonabarabran, NSW 2357, Australia.*

4 May 2021

## ABSTRACT

We have investigated the statistical clustering properties of galaxies by calculating the 2-point galaxy correlation function from the Durham/UKST Galaxy Redshift Survey. This survey is magnitude limited to  $b_J \sim 17$ , contains  $\sim 2500$  galaxies sampled at a rate of one on three and surveys a  $\sim 4 \times 10^6 (h^{-1} \text{Mpc})^3$  volume of space. We have empirically determined the optimal method of estimating the 2-point correlation function from just such a magnitude limited survey. Applying our methods to this survey, we find that our redshift space results agree well with those from previous optical surveys. In particular, we confirm the previously claimed detections of large scale power out to  $\sim 40 h^{-1} \text{Mpc}$  scales. We compare with two common models of cosmological structure formation and find that our 2-point correlation function has power significantly in excess of the standard cold dark matter model in the  $10\text{--}30 h^{-1} \text{Mpc}$  region. We therefore support the observational results of the APM galaxy survey. Given that only the redshift space clustering can be measured directly we use standard modelling methods and indirectly estimate the real space 2-point correlation function. This real space 2-point correlation function has a lower amplitude than the redshift space one but a steeper slope.

**Key words:** galaxies: clusters – galaxies: general – cosmology: observations – large-scale structure of Universe.

## 1 INTRODUCTION

Historically, the spatial 2-point correlation function,  $\xi$ , has played a central role in the quantitative measurement of the strength of galaxy clustering. It provides fundamental information about the galaxy distribution in that sense that it is the Fourier transform partner of the power spectrum of the density fluctuations. This statistic is also both easy to compute, although quite laborious, and easy to understand, with a direct probabilistic interpretation (e.g. Peebles 1980).

The usual methods of estimating the spatial 2-point correlation function are either from the deprojection of the angular correlation function,  $w(\theta)$ , (Limber 1954) or by direct estimation of the observed galaxy distribution from redshift surveys (e.g. Davis & Peebles 1983). Both methods have problems; the deprojection techniques are generally unstable and require additional galaxy number-distance information, while redshift surveys (by construction) have their galaxy distance estimates distorted by the galaxy peculiar velocity field. Therefore, they measure the real space correlation function after convolution with this field.

The initial clustering results, redshift maps, etc. of the Durham/UKST Galaxy Redshift Survey were summarized in the first paper of this series (Ratcliffe et al. 1996a). In

this paper we present a detailed analysis of the 2-point correlation function clustering techniques and results from this optically selected survey. We briefly describe our survey in Section 2. The different methods of estimating the 2-point correlation function from a magnitude limited redshift survey are described and tested in Section 3. In Section 4 we use the optimal method available to estimate the galaxy 2-point correlation function from the Durham/UKST survey and compare with the results from other galaxy redshift surveys and models of structure formation. The projected 2-point correlation function is described and estimated in Section 5. Finally, we summarize our conclusions from this analysis in Section 6.

## 2 THE DURHAM/UKST GALAXY REDSHIFT SURVEY

The Durham/UKST Galaxy Redshift Survey was constructed using the FLAIR fibre optic system (Parker & Watson 1995) on the 1.2m UK Schmidt Telescope at Sidling Spring, Australia. This survey uses the astrometry and photometry from the Edinburgh/Durham Southern Galaxy Catalogue (EDSGC; Collins, Heydon-Dumbleton

arXiv:astro-ph/9702227v1 26 Feb 1997

& MacGillivray 1988; Collins, Nichol & Lumsden 1992) and was completed in 1995 after a 3-yr observing programme. The survey itself covers a  $\sim 20^\circ \times 75^\circ$  area centered on the South Galactic Pole (60 UKST plates) and is sparse sampled at a rate of one in three of the galaxies to  $b_J \simeq 17$  mag. The resulting survey contains  $\sim 2500$  redshifts, probes to a depth greater than  $300h^{-1}\text{Mpc}$ , with a median depth of  $\sim 150h^{-1}\text{Mpc}$ , and surveys a volume of space  $\sim 4 \times 10^6 (h^{-1}\text{Mpc})^3$ .

The survey is  $>75$  per cent complete to the nominal magnitude limit of  $b_J = 17.0$  mag. This incompleteness was mainly caused by poor observing conditions, intrinsically low throughput fibres and other various observational effects. In a comparison with  $\sim 150$  published galaxy velocities (Peterson et al. 1986; Fairall & Jones 1988; Metcalfe et al. 1989; da Costa et al. 1991) our measured redshifts had negligible offset and were accurate to  $\pm 150 \text{ km s}^{-1}$ . The scatter in the EDSGC magnitudes has been estimated at  $\pm 0.22$  mags (Metcalfe, Fong & Shanks 1995) for a sample of  $\sim 100$  galaxies. This scatter has been confirmed by a preliminary analysis of a larger sample of high quality CCD photometry. All of these observational details are discussed further in a forthcoming data paper (Ratcliffe et al., in preparation).

### 3 ESTIMATING THE 2-POINT CORRELATION FUNCTION FROM A MAGNITUDE LIMITED SURVEY

In a volume limited, fair sample of the Universe (where the edge effects of the galaxy survey can be neglected) an unbiased estimate of the 2-point correlation function,  $\xi(x)$ , at separation  $x$ , is given by

$$\xi(x) = \frac{DD(x)}{RR(x)} \left( \frac{\bar{n}_R}{\bar{n}_D} \right)^2 - 1, \quad (1)$$

where  $DD(x)$  and  $RR(x)$  are the data-data and random-random pair counts at separation  $x$  and  $\bar{n}_D$  &  $\bar{n}_R$  are the mean densities of the data (galaxy) & random surveys, respectively. However, for an apparent magnitude limited survey over a given fraction of the sky things are not so simple. To estimate  $\xi$  one has to deal with a falling radial number density, how best to treat the edges of the survey and the effects of being forced to calculate the mean density internally from the survey itself. These problems manifest themselves as the estimator we use to calculate  $\xi$  and the weighting we assign to each data/random point. We will take an empirical approach to the solution of this problem and investigate the different estimators and weightings equally.

#### 3.1 The Methods of Estimation

We will present results of the redshift space 2-point correlation function,  $\xi(s)$ , where the redshift space separation between two points  $i$  and  $j$  is given by

$$s = \sqrt{s_i^2 + s_j^2 - 2s_i s_j \cos \theta}, \quad (2)$$

where  $s_i$  and  $s_j$  are the comoving redshift distances of the two points separated by an angle  $\theta$  on the sky (also see Fig. 7). Therefore, we have assumed a  $q_0 = \frac{1}{2}$ ,  $\Lambda = 0$  cosmology with comoving distances given by

$$s_i = \left( \frac{2c}{H_0} \right) \left[ 1 - \frac{1}{\sqrt{1+z_i}} \right], \quad (3)$$

where  $H_0 = 100h \text{ km s}^{-1} \text{ Mpc}^{-1}$  is the Hubble constant,  $c$  is the velocity of light in  $\text{km s}^{-1}$  and  $z$  the observed redshift.

We calculate the radial selection function using standard methods involving integrals over the galaxy luminosity function (e.g. Ratcliffe et al. 1996b). Random points are then distributed radially within the survey's angular limits with a probability proportional to the radial selection function, volume element and completeness rate of the survey. For the Durham/UKST survey this means distributing points within each of the 60 UKST fields separately because not only are the magnitude limits slightly different for each field (hence the radial selection function is slightly different) but the completeness rates are also slightly different. We have checked that this method of distributing the random points does not cause any systematic biases in  $\xi$ , see Section 3.2.

We then calculate the total number of data-data (DD), data-random (DR) and random-random (RR) pair counts in the survey and bin according to the pair separation of the points in question. We choose to bin our counts in  $0.1 \text{ dex}$  bins of separation starting at  $0.1h^{-1}\text{Mpc}$ . We calculate the 2-point correlation function using three different estimators and two different weightings. The estimators investigated here are the standard estimator (e.g. Peebles 1980)

$$\xi(x) = \frac{DD(x)}{DR(x)} \left( \frac{\bar{n}_R}{\bar{n}_D} \right) - 1, \quad (4)$$

the estimator proposed by Hamilton (1993)

$$\xi(x) = \frac{DD(x)RR(x)}{DR(x)^2} - 1, \quad (5)$$

and that of Landy & Szalay (1993)

$$\xi(x) = \frac{DD(x) - 2DR(x) + RR(x)}{RR(x)}. \quad (6)$$

The two weightings investigated here are a simple unit weighting

$$w(r) = 1, \quad (7)$$

and the so-called minimum variance weighting (Efstathiou 1988; Peebles 1973; Loveday et al. 1995)

$$w(r, x) = \frac{1}{1 + 4\pi n(r)J_3(x)}, \quad (8)$$

where  $n(r)$  is the radial number density and  $J_3(x) = \int_0^x \xi(y)y^2 dy$  is the volume integral of the 2-point correlation function out to a separation  $x$ . These estimators are essentially Monte Carlo integrations over the spherical-shell shaped volumes of the bins. These methods are particularly useful at the edges of the survey where conventional integration techniques are impractical. In order to reduce statistical fluctuations we use 25-50 times as many random points as there are data points.

The standard estimator of equation 4 stood for many years as the best estimate of  $\xi$  from these types of survey, with the  $RR \rightarrow DR$  difference from equation 1 giving a better estimate for the Monte Carlo volume integration. However, this estimator is sensitive to the error in the mean density (Hamilton 1993). Estimators which are sensitive to the square of the error in the mean density are those

proposed by Hamilton (1993) and Landy & Szalay (1993). Also, while weighting each data/random point equally is the simplest method, the pair count will be dominated by the structures in the survey near the peak of the radial number density function. This weighting essentially reduces the effective volume of the survey as volumes are unequally sampled. To weight volumes equally one should weight by the inverse of the radial selection function. Unfortunately, such a weighting is dominated by the few galaxies at large distances, where the selection function is small. Following on from work pioneered by Peebles (1973), Efstathiou (1988) has proposed a weighting which provides the mathematical minimum in the estimate of the variance of  $\xi$ . This weighting turns out to be a happy medium between equal pair weighting and equal volume weighting. To use Efstathiou's (1988) weighing we need an estimate of  $\xi$ , namely the quantity we are trying to calculate. This can be achieved via iteration but in practice a  $(r_0/r)^\gamma$  power law model for  $\xi$  suffices. We use the canonical values of  $r_0 = 5.0h^{-1}\text{Mpc}$  and  $\gamma = 1.8$  (e.g. Peebles 1980). We include an upper limit of  $J_3^{max} = 5000h^{-3}\text{Mpc}^3$  in our weighting and find our estimates of  $\xi$  relatively insensitive to doubling/halving this value.

### 3.2 Testing the Methods

We have tested the reliability of the methods described in Section 3.1 using mock catalogues of the Durham/UKST survey drawn from two sets of cold dark matter (CDM)  $N$ -body simulations. These mock catalogues were constructed in redshift space using the same angular/radial selection functions and completeness rates as the actual Durham/UKST survey. The CDM models used were (Efstathiou et al. 1985; Gaztañaga & Baugh 1995; Eke et al. 1996): standard CDM with  $\Omega h = 0.5$ ,  $b = 1.6$  (SCDM); and CDM with  $\Omega h = 0.2$ ,  $b = 1$  and a cosmological constant ( $\Lambda = 0.8$ ) to ensure a spatially flat cosmology (LCDM). Each mock catalogue was selected in such a way as to sample an independent volume of space from within the simulation. Given the relative SCDM and LCDM comoving cube sizes (256 and  $378h^{-1}\text{Mpc}$ ), this implied that we could select a total of 18 SCDM mock catalogues from the 9 available SCDM simulations and 15 LCDM mock catalogues from the 5 available LCDM simulations.

Figs. 1 and 2 show the results of applying the six different estimator and weighting combinations of Section 3.1 to the SCDM and LCDM mock catalogues, respectively. The circular, square and triangular symbols denote the estimators of equations 4, 5 and 6, respectively. Also, open symbols denote the *unweighted* estimates of equation 7 while closed symbols denote the *weighted* estimates of equation 8. The dotted line on these plots is the same simple power law model and as such can be used as a reference point. The solid lines on these plots denotes the average of the actual redshift space 2-point correlation function,  $\xi(s)$ , calculated directly from the full  $N$ -body simulations (SCDM and LCDM, respectively). Given that these are fully volume limited fair samples containing  $N$  galaxies with a well defined mean density,  $\bar{n}$ , we use equation 1 and  $RR = (4\pi/3)\bar{n}N(r_{outer}^3 - r_{inner}^3)$ , where  $[r_{inner}, r_{outer}]$  defines the extent of the radial bin in question. The error bars shown are the  $1\sigma$  standard deviation obtained from the observed

scatter between the mock catalogues. We have assumed that each mock catalogue provides a statistically independent estimate of  $\xi(s)$ . Also, to aid graphical clarity we only plot alternate error bars from the three estimators.

We also constructed a set of mock catalogues with constant completeness rates in each field. The results obtained were almost identical and therefore our method of distributing the random points does indeed correct for the variable completeness rates of each field. Another set of mock catalogues were constructed in real space rather than redshift space. Again, the results obtained were very similar and therefore the conclusions of this section are independent of real and redshift space effects.

From the SCDM mock catalogue results in Fig. 1 we see that, on small scales ( $< 10h^{-1}\text{Mpc}$ ), all of the estimates can reproduce the actual  $\xi(s)$ , although the weighted estimates are more accurate and show less scatter. On large scales ( $10-100h^{-1}\text{Mpc}$ ), all of the unweighted estimates agree well but appear biased low by  $\sim 0.03$  in  $\xi$ . However, the weighted estimates trace the actual  $\xi(s)$  very well, except for the  $DD/DR - 1$  estimator. These weighted estimates also have smaller error bars than the unweighted ones, again except for the  $DD/DR - 1$  estimator. On very large ( $> 100h^{-1}\text{Mpc}$ ) scales we do not expect the mock catalogues to produce believable results given the survey geometry involved.

We draw similar conclusions from the LCDM mock catalogue results of Fig. 2. This model has both a higher amplitude on small scales and more power on large scales than the SCDM model. This time the unweighted estimates are biased low by  $\sim 0.08$  on large ( $10-100h^{-1}\text{Mpc}$ ) scales. Again, the weighted estimates trace the actual  $\xi(s)$  well on these scales. However, the weighted  $DD.RR/DR^2 - 1$  estimator very accurately describes  $\xi(s)$  on all scales and also has the smallest error bars.

### 3.3 Errors and Biases in the Estimates

The theoretical error in the 2-point correlation function on large/linear scales has been estimated by Peebles (1973); see also Kaiser (1986). Consider a wide bin containing  $N_p$  data pairs in a single radial shell with observed number density  $n(r)$ . Assuming that  $\xi$  is small ( $\ll 1$ ) then the error in  $\xi(x)$  is given by

$$\Delta\xi(x) = \frac{1 + 4\pi n(r)J_3(x)}{\sqrt{N_p}}. \quad (9)$$

This is essentially a  $\sqrt{N}$  Poisson error modified for the effects of clustering, which reduces the amount of independent information available. We measure the maximum value of  $4\pi J_3$  for the SCDM and LCDM models to be  $\sim 7000$  and  $17000h^{-3}\text{Mpc}^3$ , respectively. If we consider the survey as a whole then  $N_p \simeq n_{gal}^2$ , where  $n_{gal}$  is the total number of galaxies in the survey. This implies a minimum theoretical error of  $\Delta\xi \simeq 0.002$  and  $0.007$  in the SCDM and LCDM mock catalogues, respectively. However, in studies of QSO clustering Shanks & Boyle (1994) have empirically shown that the error in equation 9 only works well on scales where  $N_p < n_{gal}$ . On scales where  $N_p > n_{gal}$  a more realistic error estimate is given by  $\Delta\xi \simeq 1/\sqrt{n_{gal}}$ . Given that we observe  $N_p \simeq n_{gal} \simeq 2500$  on  $5-10h^{-1}\text{Mpc}$  scales, we expect a minimum error of  $\Delta\xi \simeq 0.02$  on scales larger than this.

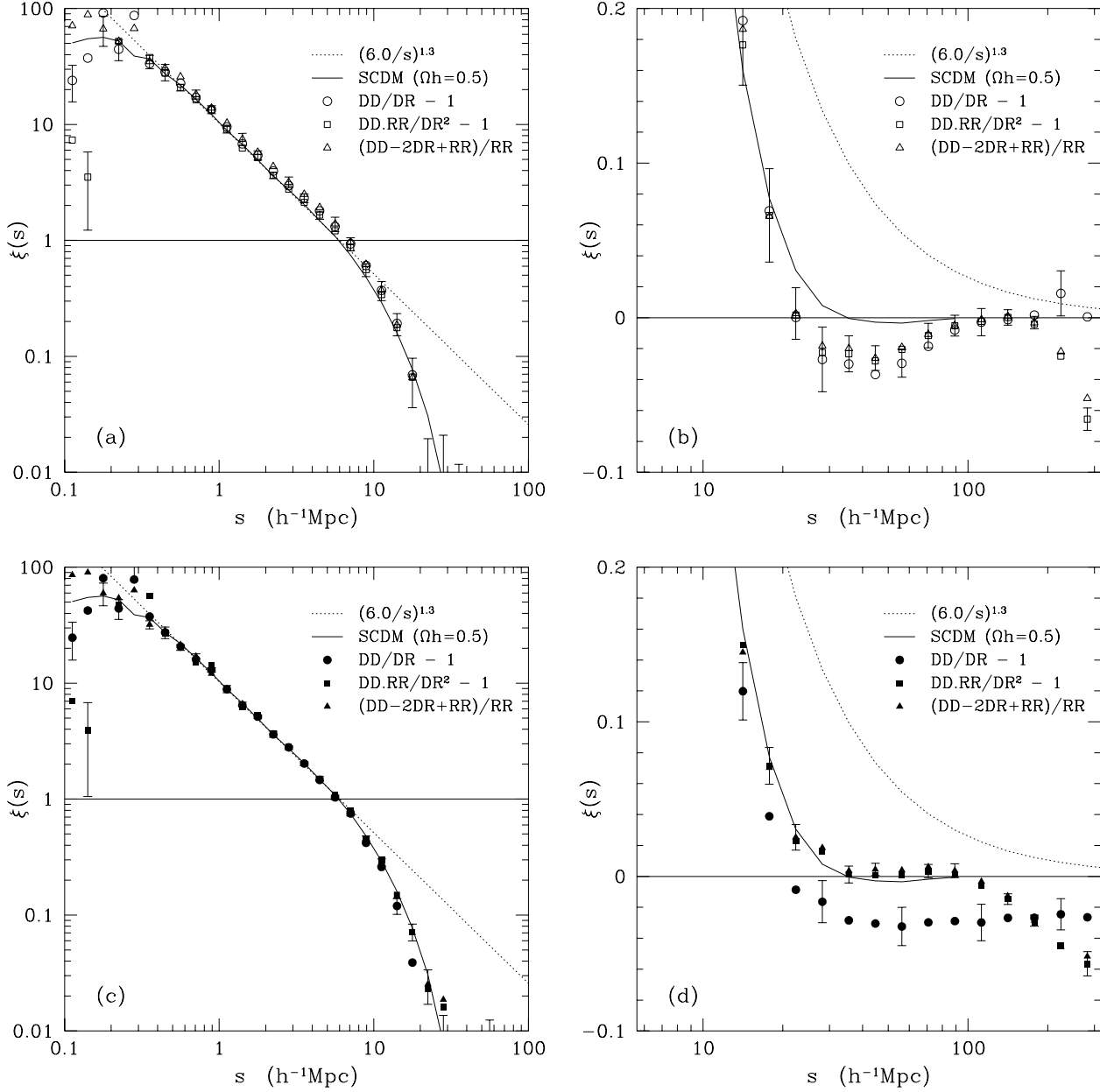


**Figure 1.** Testing the methods of estimating the redshift space 2-point correlation function,  $\xi(s)$ , from standard CDM mock catalogues which mimic the Durham/UKST survey. On all of these plots open symbols denote  $w = 1$  unweighted estimates and closed symbols denote  $w = 1/(1+4\pi n(r)J_3(x))$  weighted estimates. Also, circular, square and triangular symbols denote the estimators of equations 4, 5 and 6, respectively. Figs. (a) and (c) are plotted on a log-log scale to emphasize the small scale features, while Figs. (b) and (d) are plotted on a log-linear scale to emphasize the large scale features. The dotted line on each plot is the same simple power law model and can be used as a reference point. The solid line is the redshift space 2-point correlation function calculated directly from the  $N$ -body simulations which are used to construct the mock catalogues. Error bars are the  $1\sigma$  scatter seen between the mock catalogues assuming each one provides an independent estimate of  $\xi$ . To aid graphical clarity we plot the alternate error bars of the three estimators.

A possible bias in the estimation of  $\xi$  is due to the fact that we estimate both the mean density and the pair counts from the same survey. This leads to a non-zero difference between the true  $\xi$  of an ensemble of surveys and the ensemble average of the  $\xi$ 's from each survey. This is commonly known as the Integral Constraint (e.g. Peebles 1980) and is given by

$$I_c \simeq \frac{1 + 4\pi n(r)J_3^{max}}{n_{gal}}, \quad (10)$$

which should be added to  $\xi$  in an ensemble of surveys. One can simplify this expression by assuming  $1 \ll 4\pi n(r)J_3^{max}$  and using  $n(r) \simeq n_{gal}/V_{eff}$  to give

$$I_c \simeq \frac{4\pi J_3^{max}}{V_{eff}}, \quad (11)$$

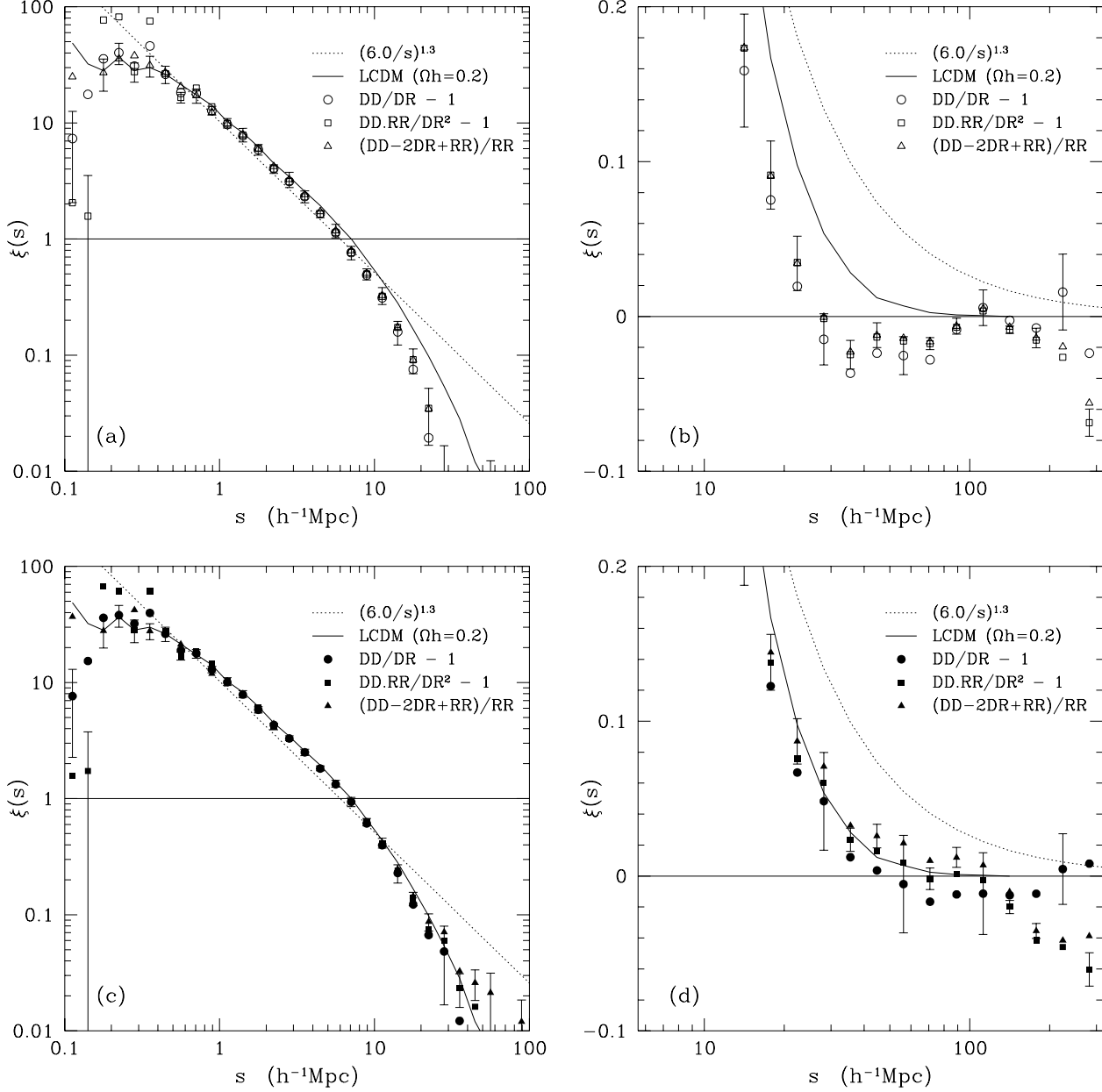


**Figure 2.** The same as Fig. 1 but for the mock catalogues constructed from the low- $\Omega$  CDM model with a non-zero  $\Lambda$  to ensure spatial flatness.

where the effective volume sampled by the survey is given by

$$V_{eff} = \int_V f(r) dV, \quad (12)$$

and  $f(r)$  is a function which reflects the weighting of the galaxies. For example, if we weight pairs equally then  $f$  is just the radial selection function, while equal volume weighting implies that  $f$  is the inverse of the radial selection function. For a typical mock catalogue we calculate  $V_{eff} \sim 2 \times 10^5 h^{-3} \text{Mpc}^3$  for equal pair weighting and  $\sim 4 \times 10^6 h^{-3} \text{Mpc}^3$  for equal volume weighting. Recalling the maximum values of  $4\pi J_3$  quoted previously we find that  $I_c \simeq 0.035$  and  $0.085$  for the SCDM and LCDM mock cat-

alogues, respectively, when using equal pair weighting and  $I_c \simeq 0.002$  and  $0.004$  when using equal volume weighting.

### 3.4 Optimal Estimate

In Section 3.3 the realistic minimum error in an *individual* mock catalogue was estimated to be  $\Delta\xi \simeq 0.02$  on large scales, for both the SCDM and LCDM models. As an example, the error bars on an individual SCDM mock catalogue are given in Figs. 3(a) and 3(b). These plots show that this is a good estimate for the errors from both the weighted and unweighted  $DD.RR/DR^2 - 1$  and  $(DD - 2DR + RR)/RR$  estimators and they asymptote towards this value on large scales ( $10\text{-}100h^{-1}\text{Mpc}$ ). How-

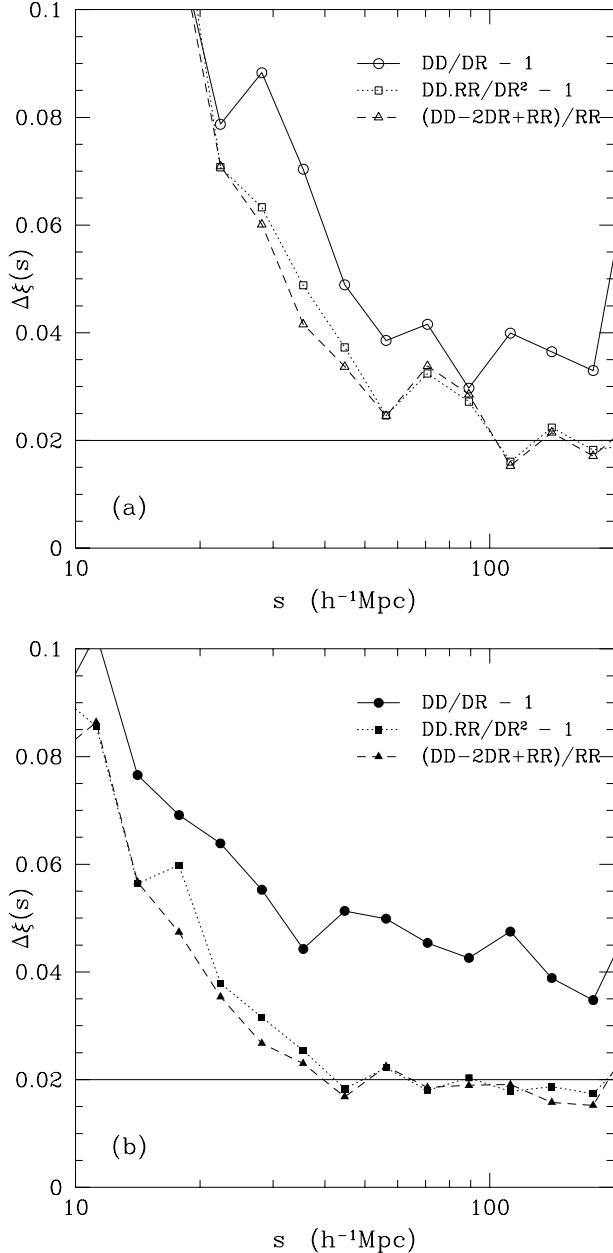


**Figure 3.** An example of the error bars ( $\Delta\xi$ ) on an individual mock catalogue for the standard CDM model. Fig. (a) shows the results from the unweighted versions of the 3 estimators, while Fig. (b) shows the corresponding weighted estimates. These error bars appear to asymptote to a value of  $\Delta\xi \simeq 0.02$  on the larger scales, in good agreement with our estimated minimum possible error bar. Very similar results were found for the LCDM model.

ever, the most consistently small error bars are given by the weighted  $DD.RR/DR^2 - 1$  and  $(DD - 2DR + RR)/RR$  estimators.

We can also compare any systematic biases in the estimates of Figs. 1 and 2 with the predicted Integral Constraint from Section 3.3. We see that all of the unweighted estimates suffer from a systematic bias which is in good agreement with the predictions from the Integral Constraint:  $\sim 0.03$  compared with  $0.035$  for the SCDM mock catalogues;

and  $\sim 0.08$  compared with  $0.085$  for the LCDM mock catalogues. For the weighted estimates there is no noticeable Integral Constraint for either set of mock catalogues for the  $DD.RR/DR^2 - 1$  and  $(DD - 2DR + RR)/RR$  estimators. Again, this is in good agreement with the small value predicted, namely  $\leq 0.005$ . We note that the weighted  $DD.RR/DR^2 - 1$  estimate most accurately reproduces the actual  $\xi$  of both the SCDM and LCDM models on all scales.

Given the historical importance of the standard  $DD/DR - 1$  estimator we briefly discuss the results obtained from it. Empirically we observe that the weighted estimate produces a larger error bar than the unweighted estimate. This is in direct contradiction with the fact that this weighting was constructed in order to produce the minimum variance in  $\xi$ . This is only seen in the  $DD/DR - 1$  estimates and therefore could be due to the estimator itself. This is possibly related to the fact that this estimator is sensitive to the error in the mean density which is different from the other estimators which are sensitive to the square of this error. Also, while the systematic bias in the unweighted estimate can be explained by the Integral Constraint, the observed bias in the weighted estimate remains unexplained. These results involving the  $DD/DR - 1$  estimator are in good agreement with a similar study of pencil-beam surveys carried out by Fong, Hale-Sutton & Shanks (1991).

To conclude this section we answer the question about which weighting and estimator combination used on a mock catalogue optimally reproduces the actual 2-point correlation function. We have found that all of our estimates appear limited by a minimum error bar which comes directly from the number of galaxies in the survey. Also, the unweighted estimates of  $\xi$  are all systematically biased low by an amount predicted by the Integral Constraint. This is due to the fact that this equal pair weighting reduces the effective volume of the survey. Finally, we see that the weighting/estimator combination which most accurately traces the actual  $\xi$  and has the smallest error bars is given by the  $w = 1/(1 + 4\pi n(r)J_3(x))$  weighting of Efstathiou (1988) and the  $DD.RR/DR^2 - 1$  estimator of Hamilton (1993). This is what we call our optimal estimate of  $\xi$  from a magnitude limited redshift survey.

## 4 THE REDSHIFT SPACE GALAXY 2-POINT CORRELATION FUNCTION

We estimate the redshift space 2-point correlation function,  $\xi(s)$ , using the methods described in Section 3. We use the magnitude limits described in Ratcliffe et al. (1996b) which maximize depth and minimize observational incompleteness in the survey. Using these limits we have  $\langle m_{lim} \rangle = 16.86 \pm 0.25$  with an average completeness rate of 75 per cent. Section 3 showed that the methods of estimation were able to account for the effects of having a slightly different magnitude limit and completeness rate in each of the 60 UKST fields.

### 4.1 Results from the Durham/UKST Survey

Fig. 4 shows the results of applying these methods to the Durham/UKST Galaxy Redshift Survey. We use Hamilton's (1993)  $DD.RR/DR^2 - 1$  estimator but show the results from

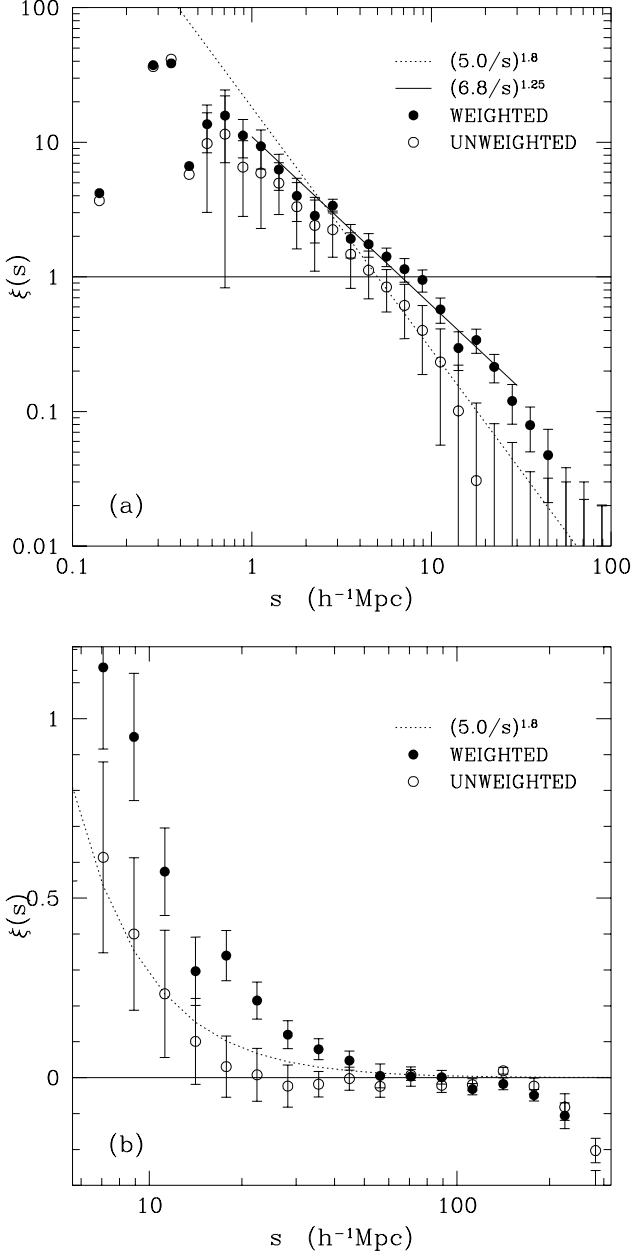


**Figure 4.** Estimates of the redshift space 2-point correlation function,  $\xi(s)$ , from the Durham/UKST Galaxy Redshift Survey using Hamilton’s (1993) estimator. Figs. (a) and (b) are plotted on log-log and log-linear scales to emphasize the small and large scale features, respectively. Open symbols denote the unweighted estimate and solid symbols denote the weighted one. The dotted line shows the canonical power law model, while the solid line shows the best fitting power law model to the weighted  $\xi(s)$  in the indicated range.

both the  $w = 1$  unweighted and the  $w = 1/(1+4\pi n(r)J_3(x))$  weighted estimates for clarity. Figs. 4(a) and 4(b) are plotted on log-log and log-linear scales to emphasize the small and large scale features, respectively. Open symbols denote the unweighted estimate and solid symbols denote the weighted one. The dotted line shows the canonical power law model for  $\xi$  of  $(5.0h^{-1}\text{Mpc}/s)^{1.8}$ , while the solid line shows the

**Table 1.** Comparison of the best fit redshift space 2-point correlation function parameters from the Durham/UKST survey with recent galaxy redshift survey results and also previous Durham ones.

Survey	$s_0$ ( $h^{-1}\text{Mpc}$ )	$\gamma$
Durham/UKST	$6.8 \pm 0.3$	$1.25 \pm 0.06$
APM-Stromlo	$5.9 \pm 0.3$	$1.47 \pm 0.12$
Las Campanas	$6.8 \pm 1.1$	$1.70 \pm 0.11$
DARS/SAAO	$6.5 \pm 0.5$	(1.8)

best fitting power law model to the weighted  $\xi(s)$  in the  $1-30h^{-1}\text{Mpc}$  range. The error bars shown are the  $1\sigma$  standard deviation on an individual low- $\Omega + \Lambda$  CDM mock catalogue (LCDM). Obviously, these error bars use the same weighting/estimator combination as the data points in question.

On all scales smaller than  $\sim 100h^{-1}\text{Mpc}$  we see that the unweighted estimate is systematically lower than the weighted one. We have tested to see if this could be explained by any systematic errors in the photometry, the method of incompleteness correction or the errors in the measured redshifts and found a negative result. It appears, quite simply, to be caused by the different weightings used. Therefore, it is thought to be partially statistical and partially due to the Integral Constraint. Indeed, using the value of  $J_3^{max}$  estimated from the weighted  $\xi(s)$  in Fig. 4 we find that equal pair weighting could cause an Integral Constraint of  $\sim 0.25$  in  $\xi$ . This is large enough to explain all of the observed difference on  $> 10h^{-1}\text{Mpc}$  scales. Equal volume weighting has an estimated Integral Constraint of  $\sim 0.01$  and is therefore not a problem for the weighted estimate. We fit our power law model using a minimum  $\chi^2$  statistic and the best fit parameters are presented in Table 1. This gave a  $\chi^2$  of  $\sim 10$  for 13 degrees of freedom, which is an adequate fit. Errors on these parameters come from the appropriate  $\Delta\chi^2$  contour about this minimum. However, given the correlated nature of these points, we anticipate that our quoted errors are more than likely an underestimate. This should be adequate for the simple comparison done here.

Finally, given the results of Section 3, we favour the weighted  $\xi(s)$  presented here as our best estimate of the redshift space 2-point correlation function.

#### 4.2 Comparison with other Redshift Surveys

Table 1 also gives a comparison of the best fit power law parameters of the  $\xi(s)$  estimated from some recent optical galaxy redshift surveys (Loveday et al. 1992, 1995; Tucker et al. 1996) and also previous Durham ones (Shanks et al. 1983, 1989). We see that the best fit redshift space correlation lengths,  $s_0$ , all agree well with a value of  $\sim 6.5h^{-1}\text{Mpc}$ . However, the slopes,  $\gamma$ , all differ significantly given the quoted error bars. (Note that the DARS/SAAO survey had  $\gamma$  fixed at 1.8 during the fitting.) Therefore, while the amplitude of  $\xi(s)$  appears well determined, there is considerable scatter in the value of the redshift space slope from the currently available data sets.

The results from these surveys are directly compared in Figs. 5(a) and 5(b) where they are plotted on log-log and log-linear scales to emphasize the small and large scale features, respectively. The error bars shown on the Durham/UKST

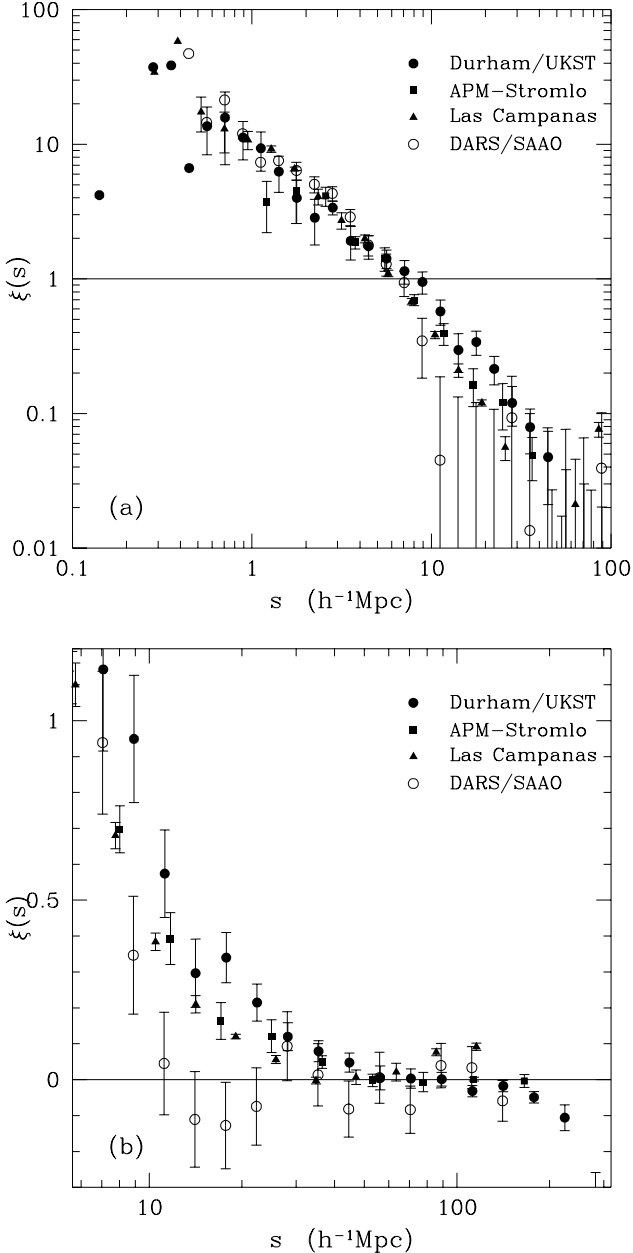


**Figure 5.** Comparison of the Durham/UKST redshift space 2-point correlation function,  $\xi(s)$ , with that from recent optical galaxy redshift surveys (Loveday et al. 1992, 1995; Tucker et al. 1996) and previous Durham surveys (Shanks et al. 1983, 1989). Figs. (a) and (b) are plotted on log-log and log-linear scales to emphasize the small and large scale features, respectively.

estimate are again those from LCDM mock catalogues. On small scales ( $< 10h^{-1}\text{Mpc}$ ) we see that all of the estimates are very consistent. On larger scales ( $> 10h^{-1}\text{Mpc}$ ) we see that the new Durham/UKST estimate agrees well with the previously claimed detections of large scale power out to  $\sim 40h^{-1}\text{Mpc}$  by the APM-Stromlo and Las Campanas surveys. On even larger scales ( $> 50h^{-1}\text{Mpc}$ ) all of the surveys are consistent with zero. All of these  $\xi$ 's use the estimator of Hamilton (1993) and the weighting of Efstathiou (1988), apart from the previous Durham DARS/SAAO re-

sults. These authors used the  $DD/DR - 1$  estimator with a  $w = 1$  weighting, but they did test against the possibility that the integral constraint could be as large as implied by the  $w(\theta)$  found from the APM survey. Also, Fong et al. (1991) tested the effect of volume weighting the DARS/SAAO data and found that the correlation function estimate only rose slightly; they also found the increase in error from the combined use of volume weighting and the  $DD/DR - 1$  estimator now reproduced in our analysis here (see Fig. 5). Hence, we conclude that the reason that the DARS/SAAO results are biased low is partly due to the use of equal pair weighting but mainly due to statistical fluctuations in the early redshift survey data.

Our conclusions from Table 1 and Fig. 5 are that a simple, one power law model does not give a good fit to the present data sets. However, the actual results from the different surveys do in fact agree well on all scales on a qualitative level, except for the DARS/SAAO results (which has large systematic errors).

### 4.3 Comparison with Structure Formation Models

We compare the redshift space 2-point correlation function from the Durham/UKST survey with the predictions of two popular structure formation models. The models we use are those from the cold dark matter simulations of Section 3, namely the standard CDM model (SCDM) and the low- $\Omega + \Lambda$  CDM model (LCDM). Historically, the SCDM model has been the standard model of structure formation for over 10 years (e.g. Davis et al. 1985), while the LCDM model is a useful phenomenological model for recent large scale structure results (e.g. Loveday et al. 1992; Baugh & Efstathiou 1993). In Figs. 6(a) and 6(b) we plot these results on log-log and log-linear scales to emphasize the small and large scale features, respectively. The shaded areas on Fig. 6 denote the 68 per cent confidence region on an individual mock catalogue, see Figs. 1 and 2. Given that the comparison here is to see how often the CDM mock catalogues can reproduce the Durham/UKST result (i.e. what is the scatter in the CDM estimates) we do not plot error bars on the Durham/UKST estimate. For consistency, all of the results presented in this figure were calculated using the optimal weighting/estimator combination of Efstathiou (1988) and Hamilton (1993).

On small scales ( $< 10h^{-1}\text{Mpc}$ ) we see that both the CDM models agree well with the results from the Durham/UKST survey. On large scales ( $> 10h^{-1}\text{Mpc}$ ) the SCDM model shows no significant power above  $\sim 20h^{-1}\text{Mpc}$  whereas the LCDM model shows significant power out to  $\sim 30h^{-1}\text{Mpc}$ . Therefore, the Durham/UKST  $\xi(s)$  has significant power ( $> 3\sigma$ ) above and beyond the SCDM model up to  $\sim 40h^{-1}\text{Mpc}$ . While the LCDM model is more consistent with the data, it also produces too little power in this region at the  $1-2\sigma$  level. This rejection of SCDM is consistent with the findings from the APM galaxy survey (Maddox et al. 1990; Loveday et al. 1992) and the QDOT infrared redshift survey (Saunders et al. 1991).



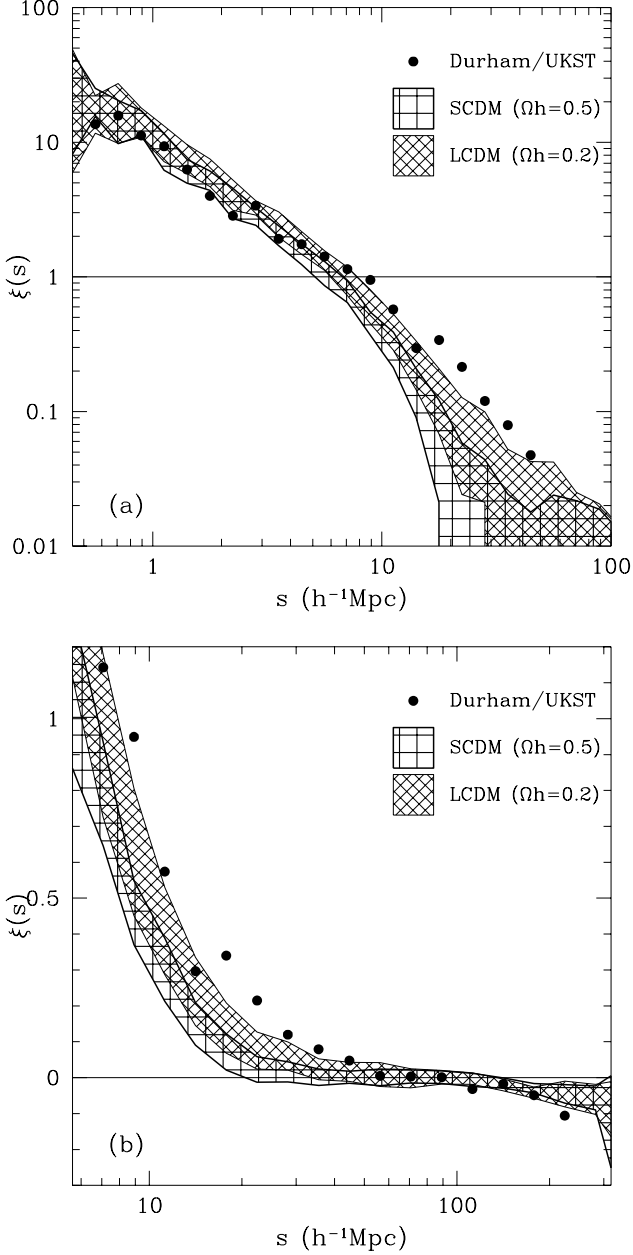


**Figure 6.** Comparison of the Durham/UKST redshift space 2-point correlation function,  $\xi(s)$ , with the results calculated from two models of structure formation, namely the standard CDM model (SCDM) and the low- $\Omega + \Lambda$  CDM model (LCDM). Mock catalogues which mimic the Durham/UKST survey were selected from the  $N$ -body simulations of these models and the shaded areas denote the 68 per cent confidence regions in  $\xi(s)$  as estimated for an individual mock catalogue. Figs. (a) and (b) are plotted on log-log and log-linear scales to emphasize the small and large scale features, respectively.

## 5 THE PROJECTED GALAXY 2-POINT CORRELATION FUNCTION

Surveys which use measured redshifts to estimate distances have the problem that the actual clustering pattern is imprinted with the galaxy peculiar velocity field. Specifically, our distance estimates are distorted by the non Hubble-flow

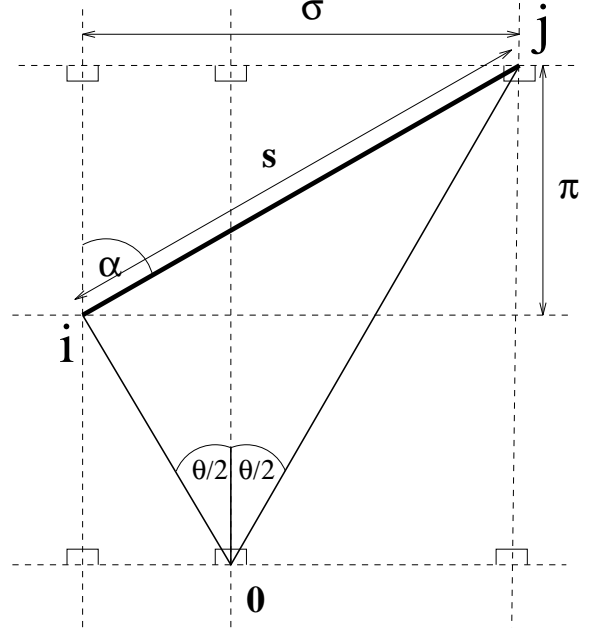


**Figure 7.** Schematic diagram to show the definitions we use to calculate the separations perpendicular ( $\sigma$ ) and parallel ( $\pi$ ) to the line of sight of two points  $i$  and  $j$ .

component of the galaxy peculiar velocity in the line of sight direction. Therefore, while our fundamental interest (in clustering terms) is in the *real* space 2-point correlation function, only the *redshift* space 2-point correlation function is directly observable from our survey. However, it is possible to model the correlation function such that we can estimate it as a simple real space power law.

We define the projected 2-point correlation function,  $w_v(\sigma)$ , by (e.g. Peebles 1980)

$$w_v(\sigma) = \int_{-\infty}^{\infty} \xi(\sigma, \pi) d\pi, \quad (13)$$

$$= 2 \int_0^{\infty} \xi(\sigma, \pi) d\pi. \quad (14)$$

where  $\xi(\sigma, \pi)$  is our usual 2-point correlation function, but calculated as a function of the separations perpendicular ( $\sigma$ ) and parallel ( $\pi$ ) to the line of sight. The definitions of  $\sigma$  and  $\pi$  we use are schematically shown in Fig. 7. We found that our results do not depend significantly on the exact nature of these definitions and even the small angle approximation gives reasonably consistent results.

### 5.1 Modelling the Projected Correlation Function

The projected nature of equation 14 allows one to write

$$w_v(\sigma) = 2 \int_0^{\infty} \xi(\sqrt{\sigma^2 + \pi^2}) d\pi, \quad (15)$$

where  $\xi(\sqrt{\sigma^2 + \pi^2})$  is the real space 2-point correlation function. Assuming a power law  $\xi(r) = (r_0/r)^\gamma$  with  $r^2 = \sigma^2 + \pi^2$  and using the definition of the Beta function gives

$$w_v(\sigma) = r_0^\gamma \left[ \frac{\Gamma(\frac{1}{2}) \Gamma(\frac{\gamma-1}{2})}{\Gamma(\frac{\gamma}{2})} \right] \sigma^{(1-\gamma)}, \quad (16)$$

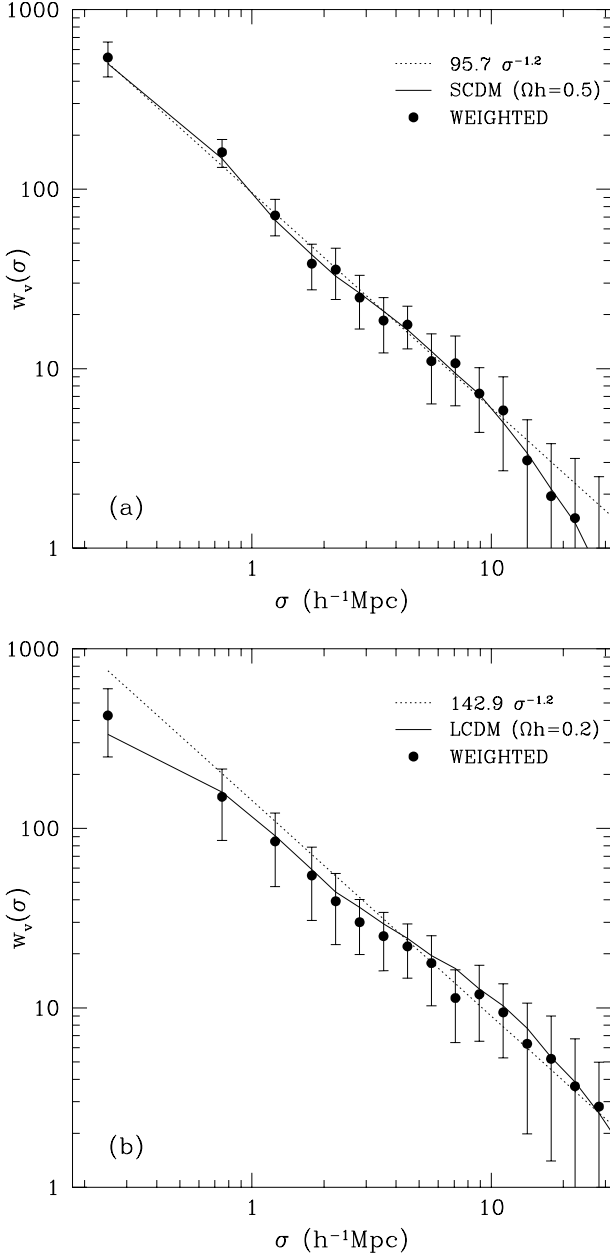


**Figure 8.** Estimates of the projected 2-point correlation function for (a) the SCDM model and (b) the LCDM model. The dotted line denotes the power law model for  $w_v(\sigma)$  predicted by equation 16. The solid line denotes the results of estimating  $w_v(\sigma)$  directly from the  $N$ -body simulations using equation 17. The solid points are the mean  $w_v(\sigma)$  for the mock catalogues as estimated from equation 17. The error bars plotted are the  $1\sigma$  standard deviation on an individual mock catalogue.

where  $\Gamma(x)$  is the Gamma function and  $\gamma > 1$  is assumed. Therefore, we can fit for our measured  $w_v(\sigma)$  to estimate a power law model of  $\xi(r)$ .

## 5.2 The Methods and Tests of the Methods

Our method for estimating  $\xi(\sigma, \pi)$  is the same as in Sections 3 and 4, except that we now bin counts in two vari-

ables instead of just one. The estimate of  $\xi(\sigma, \pi)$  becomes noisy at very large scales and so we truncate the integral in equation 14 at some upper limit,  $\pi_{cut}$

$$w_v(\sigma) = 2 \int_0^{\pi_{cut}} \xi(\sigma, \pi) d\pi. \quad (17)$$

In practise we use a  $\pi_{cut}$  of  $30h^{-1}\text{Mpc}$  for all our calculations and our results are insensitive to raising this value. This integral is carried out using a simple mid-point integration scheme which is quite adequate given the uncertainties in  $\xi(\sigma, \pi)$ .

We test these methods by using the CDM  $N$ -body simulations and mock catalogues of Section 3. Firstly, although not shown here, we have estimated the real space 2-point correlation function,  $\xi(r)$ , directly from the  $N$ -body simulations in the same manner as we estimated the actual redshift space 2-point correlation function for Figs. 1 and 2. We find that the SCDM model is approximately fit by a  $r_0 \simeq 5.0h^{-1}\text{Mpc}$ ,  $\gamma \simeq 2.2$  power law out to  $\sim 20h^{-1}\text{Mpc}$  scales. Similarly, the LCDM model has approximate parameters of  $r_0 \simeq 6.0h^{-1}\text{Mpc}$ ,  $\gamma \simeq 2.2$  out to  $\sim 30h^{-1}\text{Mpc}$  scales. These values of  $r_0$  and  $\gamma$  are then used in equation 16 to predict  $w_v(\sigma)$  power laws of  $\sim 95.7\sigma^{-1.2}$  and  $142.9\sigma^{-1.2}$  for the SCDM and LCDM models, respectively. Secondly, we estimate the redshift space  $\xi(\sigma, \pi)$  from each  $N$ -body simulation directly and average to obtain the best estimate possible for each CDM model. Using these two  $\xi(\sigma, \pi)$ 's we then estimate  $w_v(\sigma)$  from equation 17 for the SCDM and LCDM models, respectively. Finally, we estimate  $\xi(\sigma, \pi)$  from each mock catalogue using the optimal weighting/estimator combination of Efstathiou (1988) and Hamilton (1993). Many estimates of  $w_v(\sigma)$  are obtained from equation 17 and then averaged to produce the mean estimate from the SCDM and LCDM mock catalogues, respectively.

We plot these three sets of results on Fig. 8(a) for the SCDM model and Fig. 8(b) for the LCDM model. The dotted line denotes the power law model for  $w_v(\sigma)$  predicted by equation 16. The solid line denotes the results of estimating  $w_v(\sigma)$  directly from the  $N$ -body simulations using equation 17. The solid points are the mean  $w_v(\sigma)$  for the mock catalogues as estimated from equation 17. The error bars on these points are the  $1\sigma$  standard deviation on an individual mock catalogue as calculated from the scatter between the mock catalogues. Looking at Fig. 8(a) we see that the  $w_v(\sigma)$  estimated from the SCDM mock catalogues (using the optimal weighting/estimator of Section 3) does accurately reproduce the  $w_v(\sigma)$  estimated directly from the SCDM  $N$ -body simulations. Also, we see that the power law predictions of equation 16 give good agreement with the estimated  $w_v(\sigma)$  out to  $\sim 20h^{-1}\text{Mpc}$  scales, which is the scale at which the power law approximation for the SCDM  $\xi(r)$  was seen to break down in the  $N$ -body simulations. We can make similar comments regarding the LCDM results in Fig. 8(b), namely that the mock catalogues trace the expected  $w_v(\sigma)$  and the predicted power law model is a good approximation out to  $\sim 30h^{-1}\text{Mpc}$  scales, where the LCDM power law  $\xi(r)$  breaks down.

To conclude these tests of the methods we state that the mock catalogues do produce the expected projected 2-point correlation function from the  $N$ -body simulations. Also, this method can self-consistently reproduce the power law form

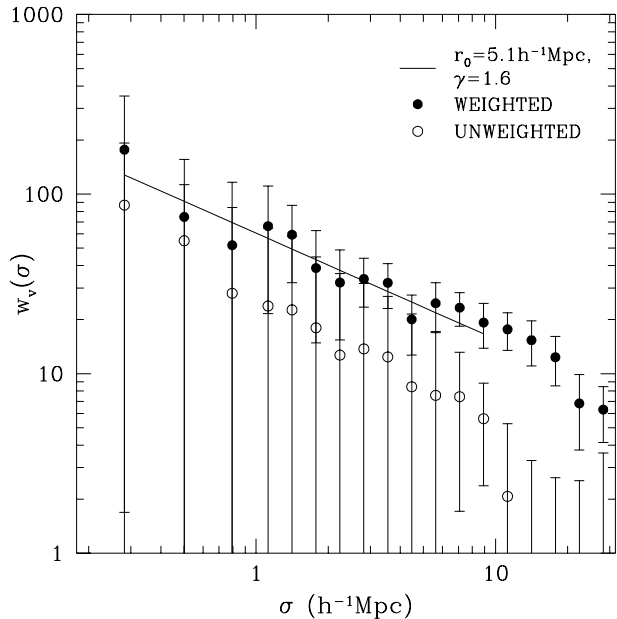


**Figure 9.** Estimates of the projected 2-point correlation function,  $w_v(\sigma)$ , from the Durham/UKST Galaxy Redshift Survey using Hamilton’s (1993) estimator. Open symbols denote the unweighted estimate while solid symbols denote the weighted one. The solid line shows the best fitting  $\xi(r)$  power law model to the weighted  $w_v(\sigma)$  in the indicated range.

of the real space 2-point correlation function from  $\xi(\sigma, \pi)$  via the projected 2-point correlation function.

### 5.3 Results from the Durham/UKST Survey

Fig. 9 shows the results of applying these methods to the Durham/UKST Galaxy Redshift Survey. We use Hamilton’s (1993)  $DD.RR/DR^2 - 1$  estimator to calculate  $\xi(\sigma, \pi)$  but, for clarity, show the results for both the unweighted estimate of equation 7 (open symbols) and the weighted estimate of equation 8 (solid symbols). The solid line shows the best fitting power law model from equation 16 to the weighted  $w_v(\sigma)$  in the  $0.25\text{--}10h^{-1}\text{Mpc}$  range. The error bars shown are the  $1\sigma$  standard deviation on an individual LCDM mock catalogue. Obviously, these error bars use the same weighting/estimator combination as the data points in question.

We see that the unweighted estimate is systematically lower than the weighted one. This is a direct result of the weighted redshift space 2-point correlation function being higher than the unweighted one (see Fig. 4). The power law approximation of equation 16 is fit using a minimum  $\chi^2$  statistic and the best fit parameters are presented in Table 2. This gave a  $\chi^2$  of  $\sim 8$  for 12 degrees of freedom, which is an adequate fit. Errors on these parameters come from the appropriate  $\Delta\chi^2$  contour about this minimum. However, given the correlated nature of these points, we anticipate that our quoted errors are more than likely an underestimate. Again, this should be adequate for the simple comparison done here.

Table 2 also gives a comparison of the best fit  $\xi(r)$  power law model parameters to the  $w_v(\sigma)$  estimated from some recent optical galaxy redshift surveys (Loveday et al. 1995; Lin et al. 1996) and also previous Durham ones (Bean et al.

**Table 2.** Comparison of the best fit real space 2-point correlation function parameters from the Durham/UKST survey with recent galaxy redshift survey results and also previous Durham ones.

Survey	$r_0$ ( $h^{-1}\text{Mpc}$ )	$\gamma$
Durham/UKST	$5.1 \pm 0.3$	$1.60 \pm 0.10$
APM-Stromlo	$5.1 \pm 0.2$	$1.71 \pm 0.05$
Las Campanas	$5.0 \pm 0.14$	$1.79 \pm 0.04$
DARS/SAAO	$4.7 \pm 0.4$	(1.8)

1983; Hale-Sutton et al. 1989). We see that the best fit real space correlation lengths,  $r_0$ , all agree well with a value of  $\sim 5.0h^{-1}\text{Mpc}$ . Also, the slopes,  $\gamma$ , all agree quite well with a value of  $\sim 1.75$ , bar the Durham/UKST one which is  $1\text{--}2\sigma$  low. (Again the DARS/SAAO survey had  $\gamma$  fixed at 1.8 during the fitting.) We find consistent results when comparing with the  $r_0 \simeq 4.5h^{-1}\text{Mpc}$  and  $\gamma \simeq 1.7$  obtained by Baugh (1996) from numerically inverting the APM angular correlation function,  $w(\theta)$ .

Our conclusion from Table 1 is that a simple one power law model gives both an adequate fit and consistent results from present data sets.

## 6 CONCLUSIONS

We have empirically determined the optimal method of estimating the 2-point correlation function from a magnitude limited galaxy redshift survey. Our method used Monte Carlo techniques on mock catalogues drawn from  $N$ -body simulations of cold dark matter structure formation models. From the currently available choices of 2-point correlation function estimator and weighting we find that both the minimum variance and most accurate reproduction of the 2-point correlation function is given by the estimator of Hamilton (1993) and the weighting of Efstathiou (1988).

These techniques are then applied to the Durham/UKST Galaxy Redshift Survey and the redshift space 2-point correlation function is calculated for this survey. We find that our results agree well with those from other recent redshift surveys and confirm the previously claimed detections of large scale power in the  $10\text{--}40h^{-1}\text{Mpc}$  regime (e.g. Loveday et al. 1992, 1995). A simple power law model is an adequate fit to the data (although not particularly impressive) and has redshift space parameters of correlation length,  $r_0 = 6.8 \pm 0.3h^{-1}\text{Mpc}$ , and slope,  $\gamma = -1.25 \pm 0.06$ . At small scales these results agree with the results from previous Durham pencil-beam surveys (Shanks et al. 1983, 1989). However, at large ( $r > 10h^{-1}\text{Mpc}$ ) scales the older surveys suggested too little power, mainly due to statistical fluctuations, with some smaller contribution due to integral constraint.

We compare our results with the predictions of two common models of structure formation, namely the standard cold dark matter model,  $\Omega h = 0.5$  &  $b = 1.6$  (SCDM), and a low density cold dark matter model with a non-zero cosmological constant to ensure spatial flatness,  $\Omega h = 0.2$ ,  $\Lambda = 0.8$  &  $b = 1.0$  (LCDM). Our results agree well with both of these models on small scales  $< 10h^{-1}\text{Mpc}$  but on larger scales we find our results are  $> 3\sigma$  above and beyond the SCDM model in the  $10\text{--}40h^{-1}\text{Mpc}$  regime. The LCDM

model is more consistent with our results but is still  $1-2\sigma$  low.

Given that our survey uses redshifts as distance estimates our measured clustering statistics are distorted by the peculiar velocity field. Using standard techniques (e.g. Peebles 1980) we calculate the projected 2-point correlation function and use it to model the real space 2-point correlation function. We find that a simple power law model provides an adequate fit to the projected 2-point correlation function from the Durham/UKST survey which implies real space parameters of correlation length,  $r_0 = 5.1 \pm 0.3 h^{-1} \text{Mpc}$ , and slope,  $\gamma = -1.6 \pm 0.1$ . The differences seen in the real and redshift space parameters is discussed in the next paper in this series.

## ACKNOWLEDGMENTS

We are grateful to the staff at the UKST and AAO for their assistance in the gathering of the observations. S.M. Cole, C.M. Baugh and V.R. Eke are thanked for useful discussions and supplying the CDM simulations. AR acknowledges the receipt of a PPARC Research Studentship and PPARC are also thanked for allocating the observing time via PATT and for the use of the STARLINK computer facilities.

## REFERENCES

- Baugh C.M., 1996, MNRAS, 280, 267  
 Baugh C.M., Efstathiou G., 1993, MNRAS, 265, 145  
 Bean A.J., Efstathiou G., Ellis R.S., Peterson B.A., Shanks T., 1983, MNRAS, 205, 605  
 Collins C.A., Heydon-Dumbleton N.H., MacGillivray H.T., 1988, MNRAS, 236, 7P  
 Collins C.A., Nichol R.C., Lumsden S.L., 1992, MNRAS, 254, 295  
 da Costa L.N., Pellegrini P.S., Davis M., Meiksin A., Sargent W.L., Tonry J.L., 1991, ApJS, 75, 935  
 Davis M., Efstathiou, G., Frenk C.S., White S.D.M., 1985, ApJ, 292, 371  
 Davis M., Peebles P.J.E., 1983, ApJ, 267, 465  
 Efstathiou G., in Lawrence A., ed., 3rd *IRAS*, Conference, London, Comets to Cosmology. Springer, Berlin, p. 312  
 Efstathiou G., Davis M., Frenk C.F., White S.D.M., 1985, ApJS, 57, 241  
 Eke V.R., Cole S.M., Frenk C.S., Navarro J.F., 1996, MNRAS, 281, 703  
 Fairall A.P., Jones A., 1988, *Publs. Dept. Astr. Cape Town*, 10  
 Fong R., Hale-Sutton D., Shanks T., 1991, in Blanchard A. et al. eds., 25th Anniversary of the Cosmic Background Radiation Discovery. Editions Frontieres, France, p.289  
 Gaztañaga E. & Baugh C.M., 1995, MNRAS, 273, 1P  
 Hale-Sutton D., Fong R., Metcalfe N., Shanks T., 1995, MNRAS, 237, 569  
 Hamilton A.J.S., 1993, ApJ, 419, 19  
 Kaiser N., 1986, MNRAS, 227, 1  
 Landy S.D., Szalay A.S., 1993, ApJ, 412, 64  
 Limber D.N., 1954, ApJ, 119, 655  
 Lin H., Kirchner R.P., Tucker D.L., Shectman S.A., Landy S.D., Oemler A., Schechter P.L., 1996, submitted to ApJ  
 Loveday J., Efstathiou G., Peterson B.A., Maddox S.J., 1992, ApJ, 400, L43  
 Loveday J., Maddox S.J., Efstathiou G., Peterson B.A., 1995, ApJ, 442, 457  
 Maddox et al., 1990...  
 Metcalfe N., Fong R., Shanks T., Kilkenny D., 1989, MNRAS, 236, 207  
 Metcalfe N., Fong R., Shanks T., 1995, MNRAS, 274, 769  
 Parker Q.A., Watson F.G., 1995, in Maddox S.J., Aragón-Salamanca A., eds., 35th Herstmonceux Conf. Cambridge, Wide Field Spectroscopy and the Distant Universe. World Scientific, Singapore, p. 33  
 Peebles P.J.E., 1973, ApJ, 185, 413  
 Peebles P.J.E., 1980, *The Large-Scale Structure of the Universe*, Princeton Univ. Press, Princeton, NJ  
 Peterson B.A., Ellis R.S., Efstathiou G.P., Shanks T., Bean A.J., Fong R., Zen-Long Z., 1986, MNRAS, 221, 233  
 Ratcliffe A., Shanks T., Broadbent A., Parker Q.A., Watson F.G., Oates A.P., Fong R., Collins C.A., 1996a, MNRAS, 281, L47  
 Ratcliffe A., Shanks T., Parker Q.A., Fong R., 1996b, submitted to MNRAS  
 Saunders W., Frenk C.S., Rowan-Robinson M., Efstathiou G., Lawrence A., Kaiser N., Ellis R.S., Crawford J., Xia x.-Y., Parry I., 1991, Nat, 349, 32  
 Shanks T., Bean A.J., Efstathiou G., Ellis R.S., Fong R., Peterson B.A., 1983, ApJ, 274, 529  
 Shanks T., Boyle B.J., 1994, MNRAS, 271, 753  
 Shanks T., Hale-Sutton D., Fong R., Metcalfe N., 1989, MNRAS, 237, 589  
 Tucker D.L., Oemler A.A., Shectman S.A., Kirchner R.P., Lin H., Landy S.D., Schechter P.L., 1996, preprint.